

Particle acceleration and heating in regions of magnetic flux emergence: a statistical approach using test-particle- and MHD- simulations

H. Isliker , L. Vlahos, V. Archontis, Th. Pisokas
Dept. of Physics, University of Thessaloniki

Thessaloniki, 2015

Outline

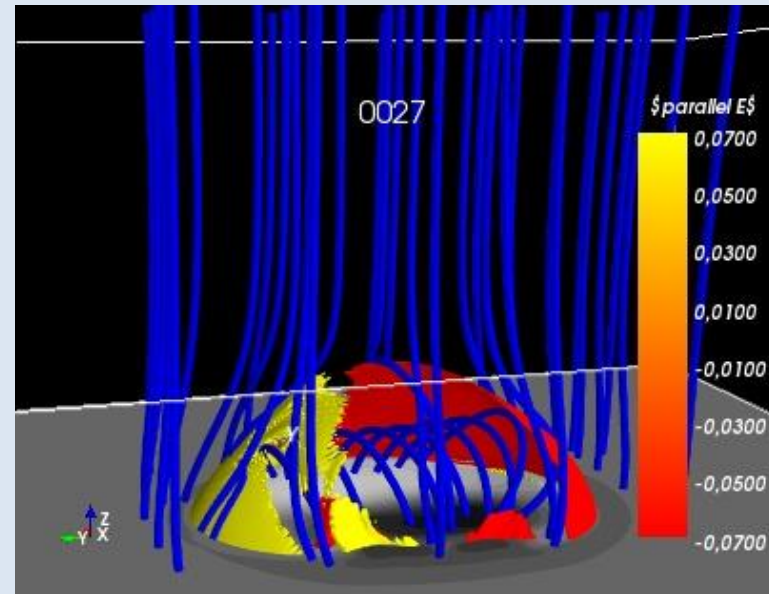
3D nonlinear MHD simulations of an emerging flux tube,
from convection zone into the corona
(Vasilis Archontis):

In this study:

- Focus on the **coronal** part
- **Spatial structure** and **statistics** of the **electric field** and other MHD quantities

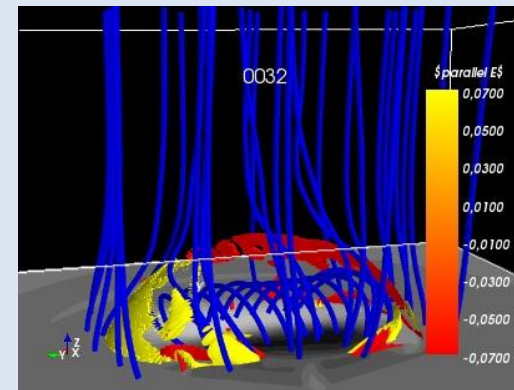
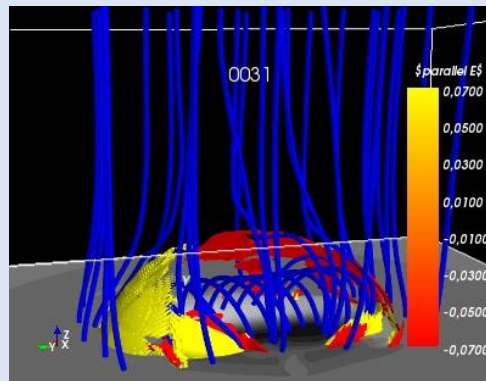
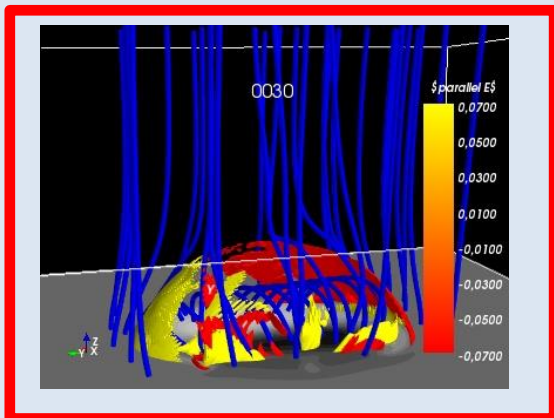
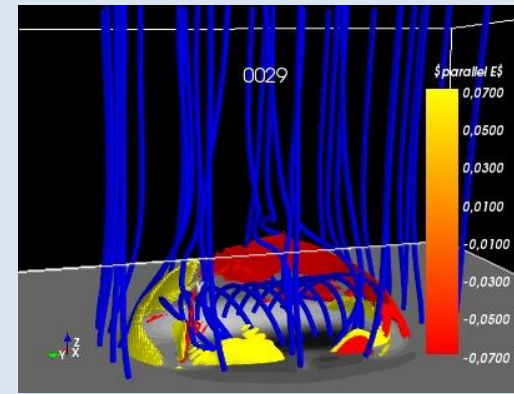
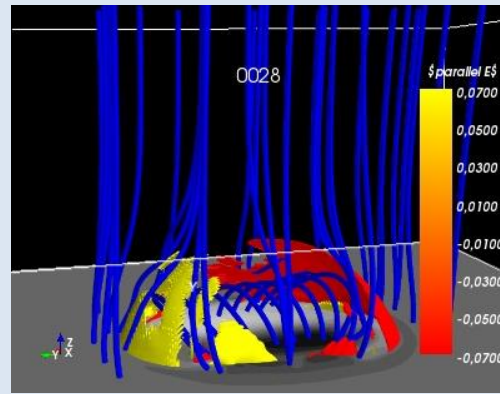
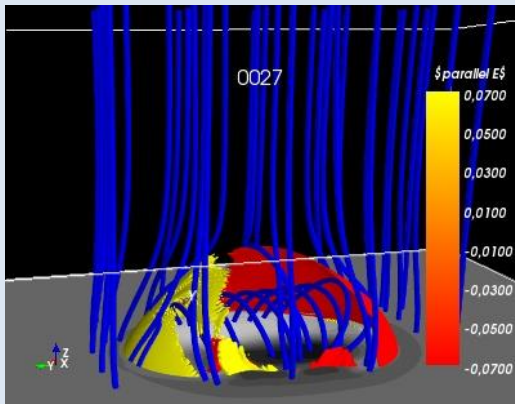
Test-particle simulations (electrons):

- **heating**
- **acceleration**
- Particular aim of this project also is to investigate the relation of the acceleration mechanism to Fermi acceleration and Fokker-Planck modeling
→ determine **transport coefficients**



MHD simulations: reconnection and standard jet

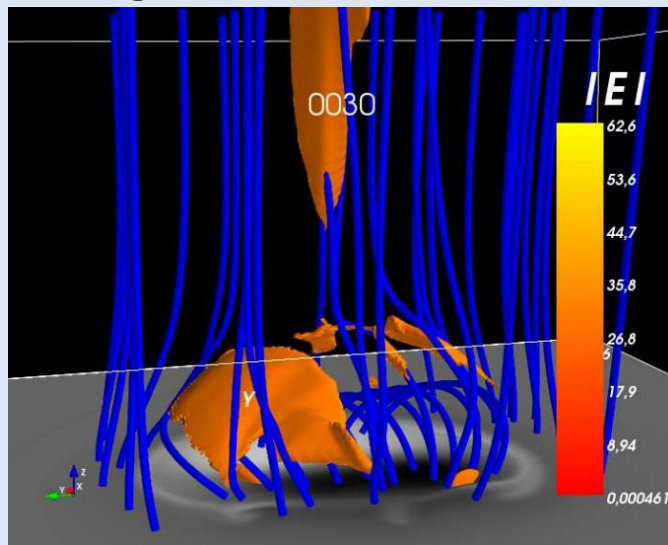
- MHD snapshots of emerging flux tube, reconnecting with pre-existing ambient coronal field:
 - 'standard' jet is formed, which is triggered by the eruption of dense and cool plasma from the emerging flux region
 - turbulence on small scales



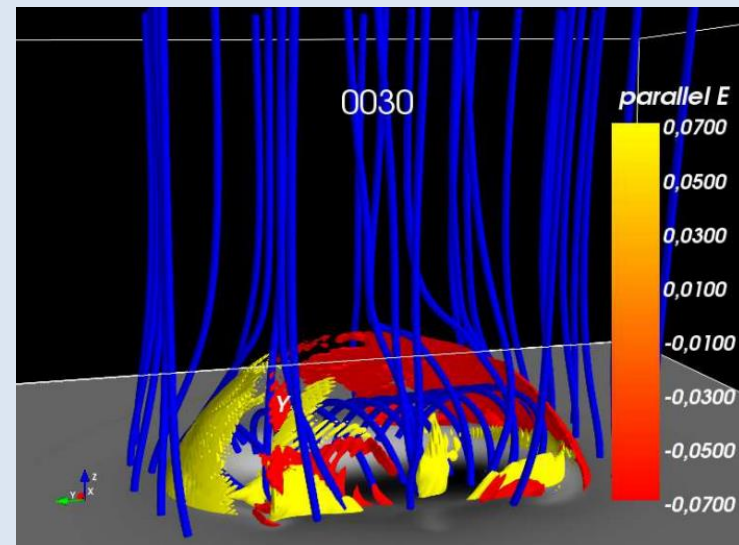
Spatial structure of the magnetic and electric field

- Snapshot 30, standard outflow jet:
- We concentrate on parallel el. field since it is dominantly responsible for acceleration, see later
- **Parallel electric field** shows fragmented structures, and has preferred regions of pos. and neg. sign

magnitude of **total el. field**



parallel el. field



- **Fragmentation** needs to be quantified: **cluster analysis, fractal dimension**

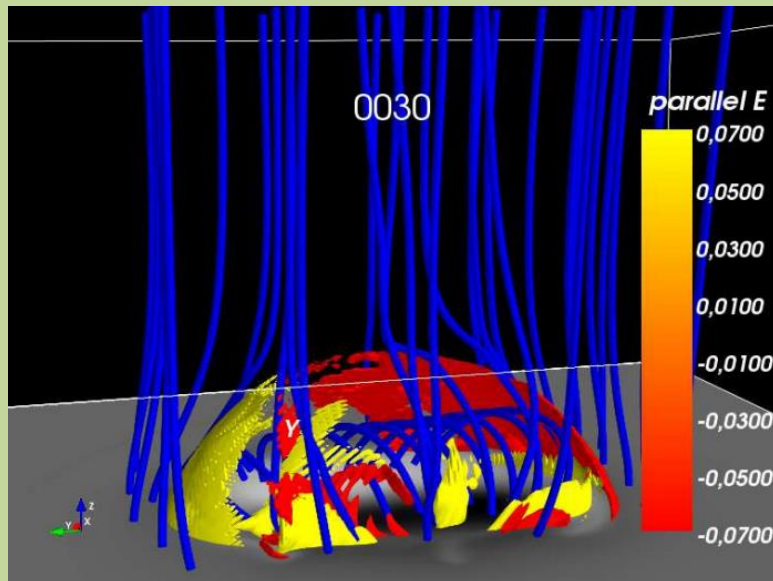
Cluster analysis of parallel electric field

Cluster defined as grid-sites with above-threshold electric field, connected through nearest neighborhood

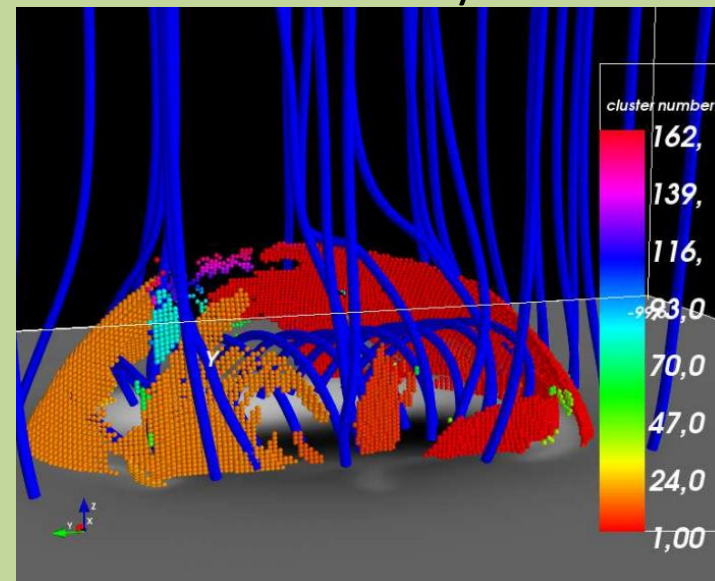
Similar to 3D iso-contour-plot, but identifies not connected regions

Free parameter: threshold 0.07, will be justified later

iso-contours



cluster analysis

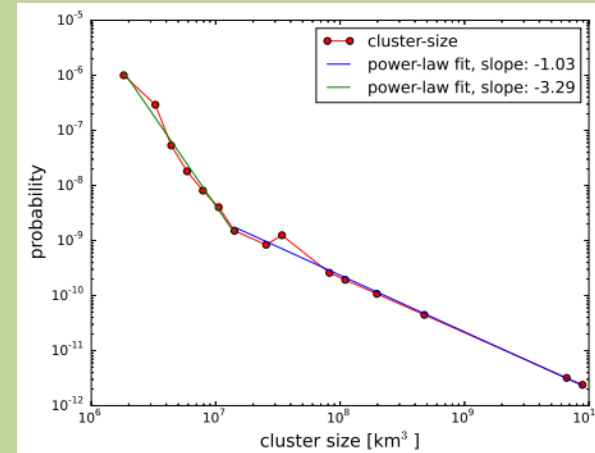


→ Cluster-size distribution

→ fractal dimension of cluster distribution

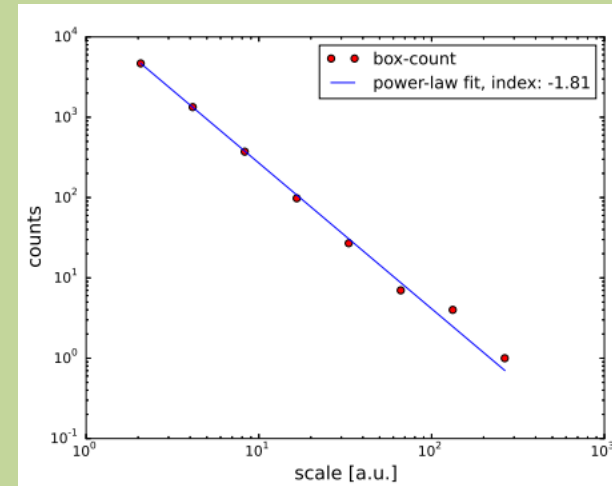
Cluster-size distribution, fractal dimension

- Cluster-size distribution, here size = number of grid-points a cluster consists of, times elementary grid-volume: double power-law



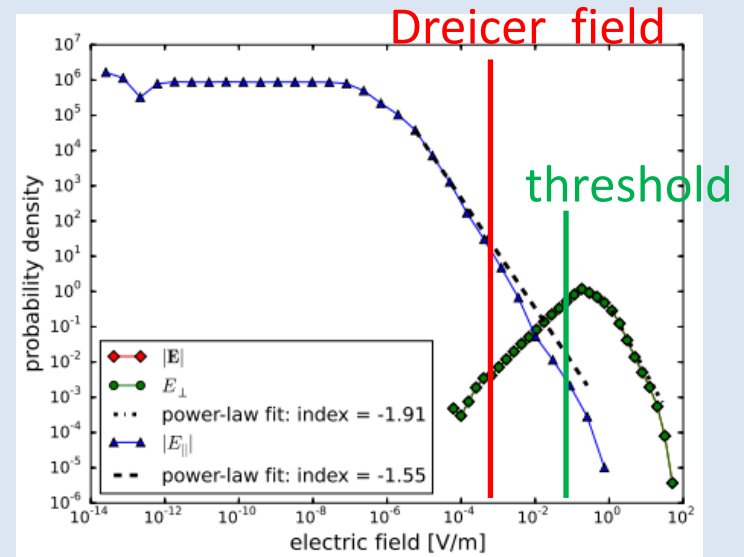
cluster-size [# grid-points* ΔV]

- Fractal dimension of clusters, box-counting method in 3D: dimension 1.8, rarified sheet-like structures → fragmented current sheets



Statistics of the electric field

- Histogram of the magnitude of the total, parallel, and perp. electric field
- Parallel el. field **100 times smaller** than perpendicular one, power-law tail, index 1.6
- Mean **Dreicer field** $E_D = 5 \times 10^{-4}$ V/m
- **Perp. el. field** clearly super-Dreicer, **parallel el. field** super-Dreicer only at a fraction of the grid-points
- **Threshold** for iso-contours, clusters, and fractal dimension: **$140 E_D$**
→ region of clearly super-Dreicer parallel el. Field.



Statistical analysis of MHD data: Energies

- Perpendicular dynamics expected to be dominated by **E cross B drift**: expected energetics

$$E_{\text{kin, EcB}} = (1/2) m_e (\mathbf{E} \text{ cross } \mathbf{B}\text{-velocity})^2$$

histogram of E_{kin} from all grid-sites:

→ power-law, index 1.3, yet maximum energy very small: 0.1 keV

→ we would expect perpendicular energization to be negligible

(note: no test particles were run for this result)

- Distribution of **MHD flow kinetic energy**

$$E_{\text{kin, B}} = (1/2) m_e V^2$$

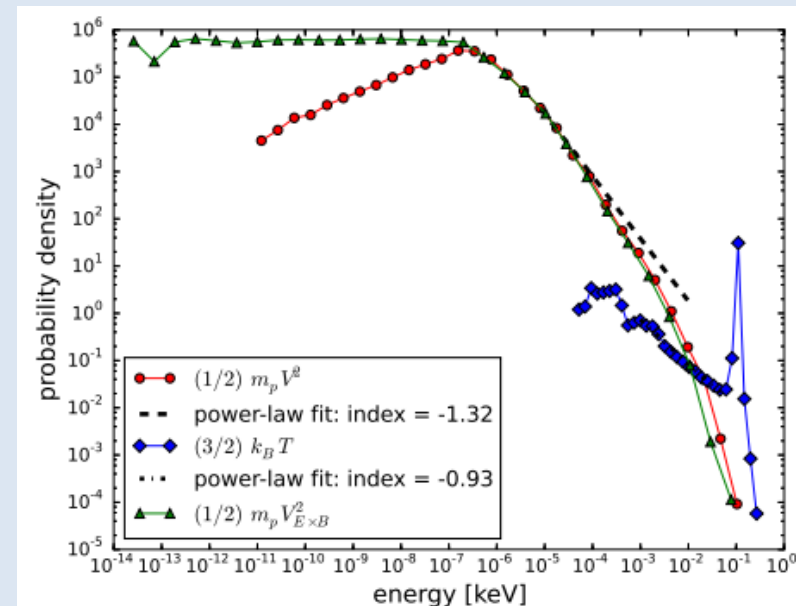
→ similar to E cross B energy

- Distribution of **MHD temperature T**

$$(3/2) k_B T$$

power-law and peak at 0.1 keV

- Maximum energies in any case 0.2 keV**



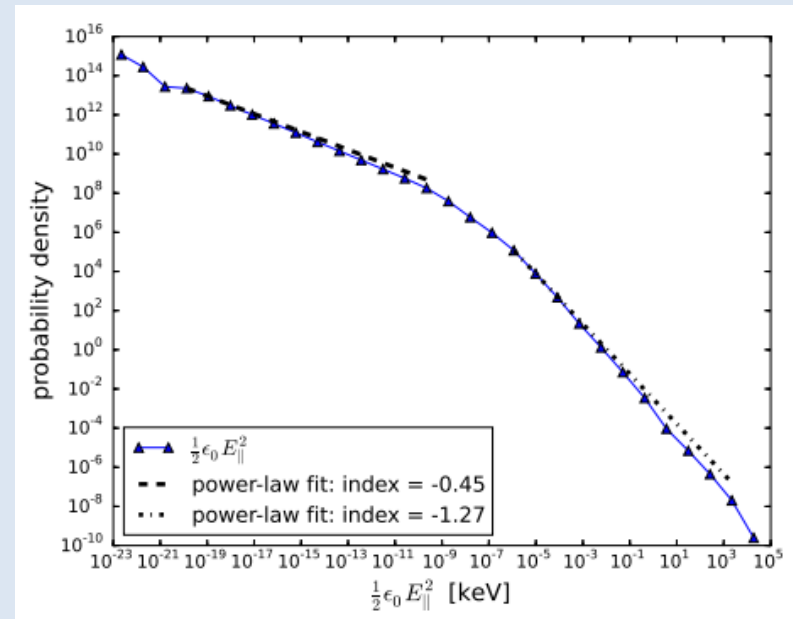
Statistical analysis of MHD data: Energies

- Distribution of the parallel electric energy:

$$W_{E_{||}} = (1/2) \epsilon_0 E_{||}^2$$

Very extended double power-law,
index 1.3 at high energies

- highest energy 20 MeV



- various power-law distributions already in MHD data !
- MHD simulation highly non-linear, far from equilibrium

Test-particle simulations: the equations of motions

- Direct, **non-linear test-particle simulations**, in 3D geometry:
MHD fields are interpolated locally with 3D, continuous cubic polynomials
- 1st order **relativistic guiding center** approximation

$$\frac{d\mathbf{r}}{dt} = \frac{1}{B_{\parallel}^*} \left[\frac{u_{\parallel}}{\gamma} \mathbf{B}^* + \hat{\mathbf{b}} \times \left(\frac{\mu}{q\gamma} \nabla B - \mathbf{E}^* \right) \right]$$

$$\frac{du_{\parallel}}{dt} = -\frac{q}{m_0 B_{\parallel}^*} \mathbf{B}^* \cdot \left(\frac{\mu}{q\gamma} \nabla B - \mathbf{E}^* \right)$$

$$\mathbf{B}^* = \mathbf{B} + \frac{m_0}{q} u_{\parallel} \nabla \times \hat{\mathbf{b}}$$

$$\mathbf{E}^* = \mathbf{E} - \frac{m_0}{q} u_{\parallel} \frac{\partial \hat{\mathbf{b}}}{\partial t}$$

$$\mu = mv_{\perp}^2 / (2B)$$

$$\hat{\mathbf{b}} = \mathbf{B} / B$$

$$\mathbf{u} = \gamma \mathbf{v}$$

$$\gamma = \frac{1}{\sqrt{1 - (v/c)^2}}$$

(Tao, Chan, & Brizard (2007), Grebogi & Littlejohn (1984))

- **Benchmarked** by comparing to integrating **Lorentz force**

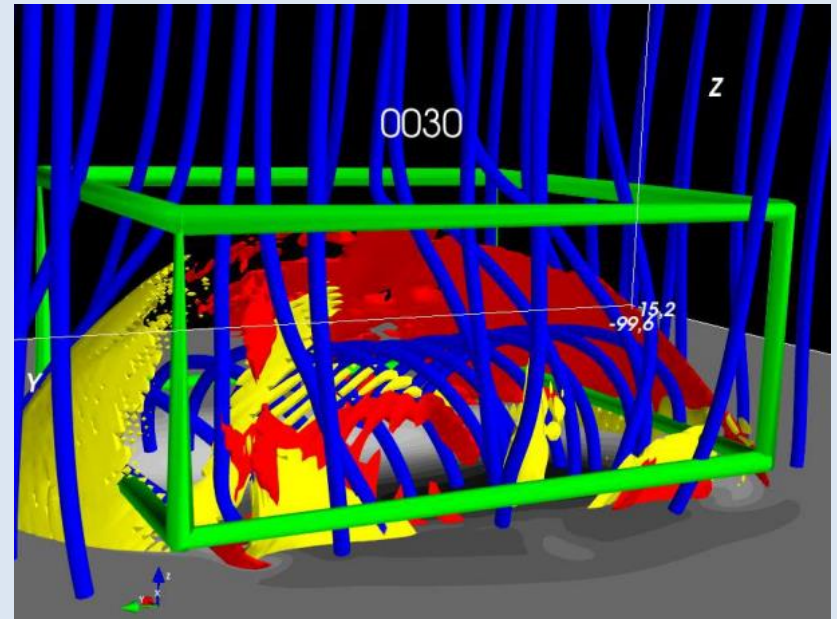
$$d\mathbf{r}/dt = \mathbf{v}, \quad d\mathbf{u}/dt = (q/m)(\mathbf{v} \times \mathbf{B} + \mathbf{E})$$

→ Very good coincidence is found

- Important: parallel electric field has to be interpolated explicitly, else artificial fields are generated !
- In any case, numerical integration with 4th order Runge Kutta, adaptive time-step scheme (version of Dormand Prince)
- The code has been **parallelized** with OpenMP and with MPI

Test-particle simulations: the set-up

- The electric and magnetic field are de-normalized to SI units and not further scaled.
- Mostly **100'000 to 500'000 electrons** are traced, and intermediate and the final kinetic energy distribution is calculated
- Final integration time mostly is **0.1 sec**:
MHD time-step = **25 sec**, so particles evolve in **fixed MHD snap-shots**
- the **initial velocity** is random Maxwellian, with temperature $\approx 9 \times 10^5$ K
- **initial position** is uniformly random in a box in the central region around the main reconnection regions

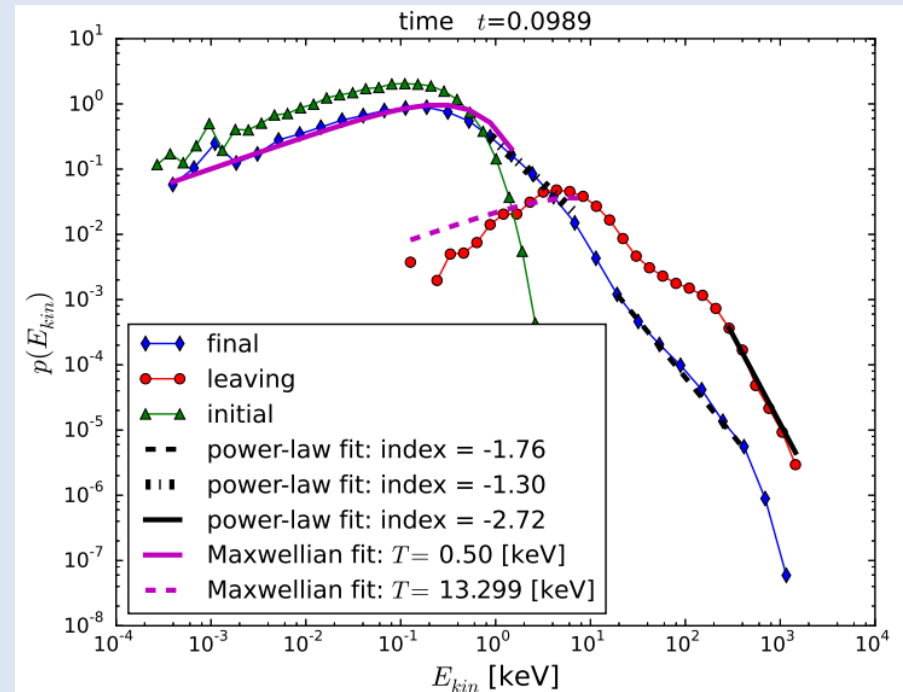


Standard jet: results at 0.1s

- The final energy distribution at 0.1s is of **Maxwellian** shape at the low energies, and exhibits a **double power-law tail**

Acceleration:

- The maximum energy reached is about **2 MeV**, and a power-law fit to the tail yields an index of about 1.30 at the lower energies and **1.76** at the higher energies.
- 13% of the 100'000 particle have left leave at 0.1 s**, and they have energies in the same range than those that stay inside, with a modulated power-law tail that is steeper though, with index 2.72 at the highest energies.



Standard jet: results at 0.1s

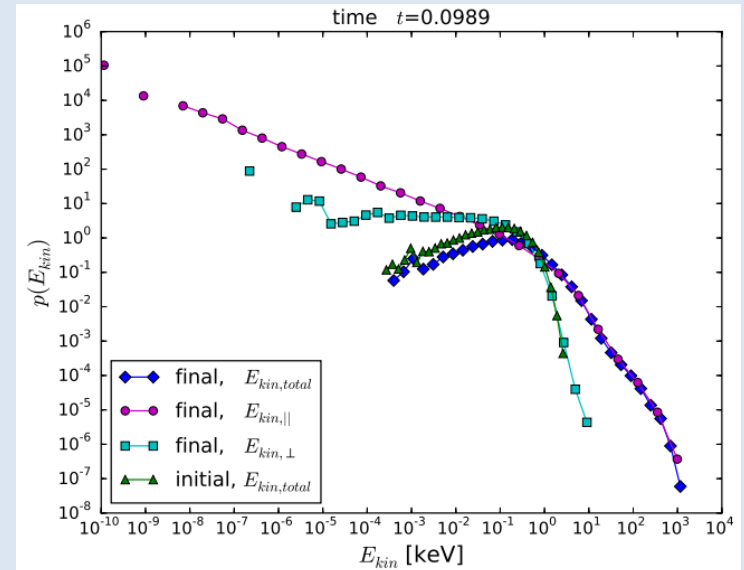
Acceleration, cont'd:

- **final total, parallel, and perpendicular kinetic energy at 0.1 s:**
 - the power-law tail in the total kinetic energy stems from the parallel kinetic energy,
 - essentially no energization in the perpendicular direction,

important conclusion:

acceleration is acting exclusively in the parallel direction.

- simulation with 10 times more particles (1'000'000): no real changes in the results, statistics is good enough



Standard jet: results at 0.1s

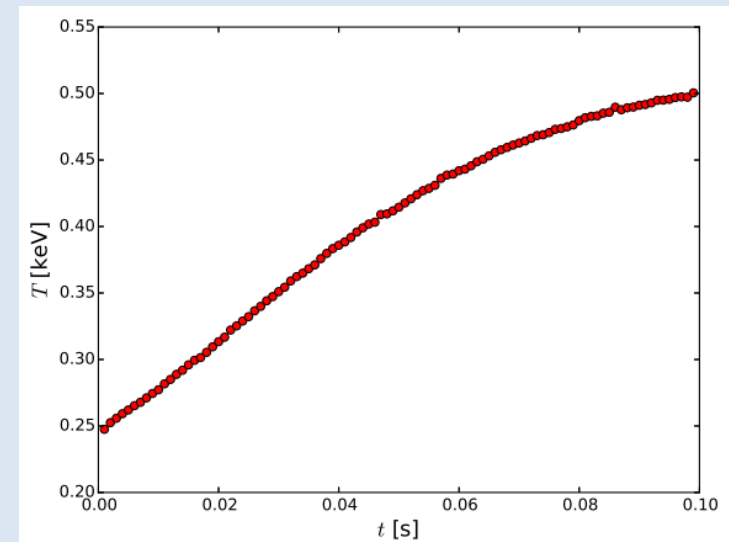
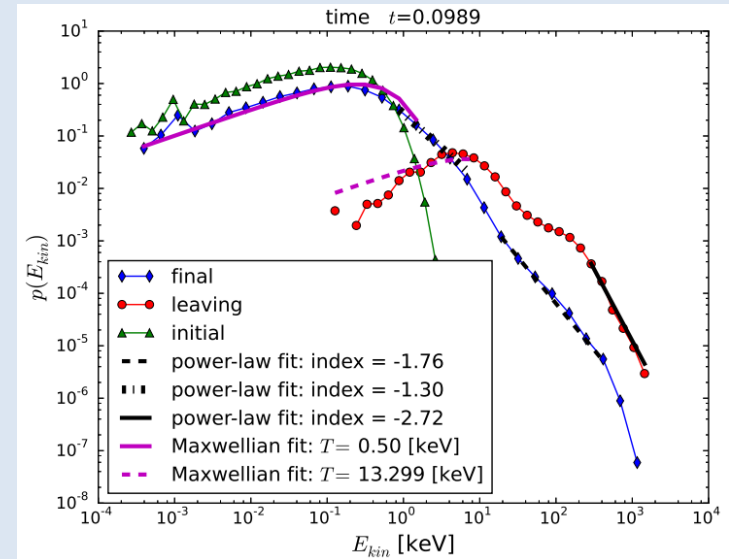
Heating:

particles that stay inside:

- Maxwellian shape of the energy distribution at low energies:
heating **from the initial 0.24 keV to 0.50 keV** (1.8MK)
- Temperature as a function of time increases linearly until 0.05 s and then starts to turn over, reaches a peak value of 0.50 keV at 0.1 s

leaving particles at low energies:

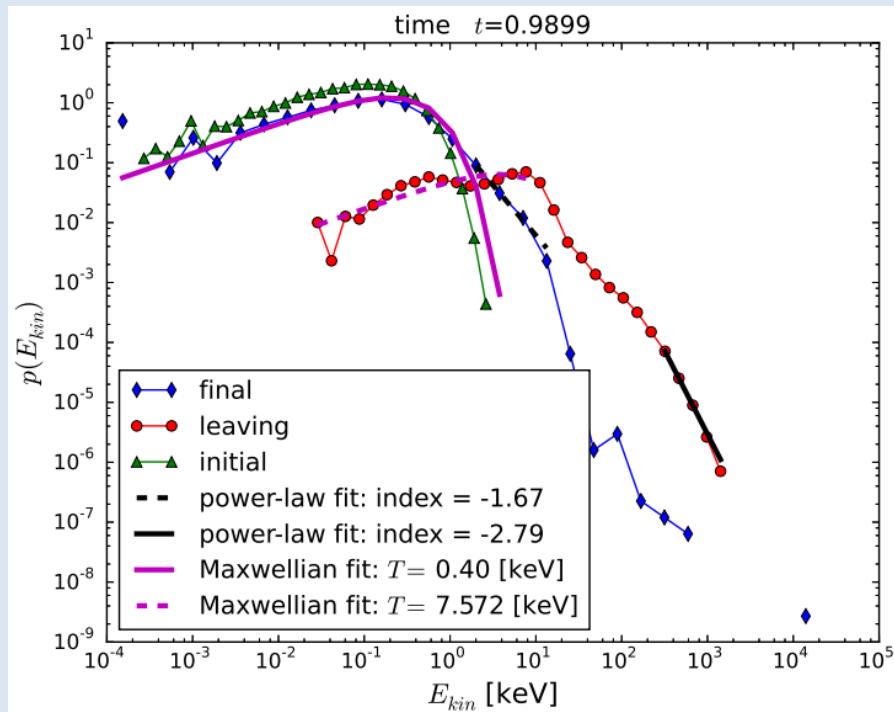
- distribution reminiscent of a Maxwellian, temperature of about 13.3 keV:
→ **super-hot population of 50 MK.** (the statistics is not very good)
- It is to note though that the energies are collected at different times for each particle.



Standard jet: results at 1.0s

Longer times: 1.0 s

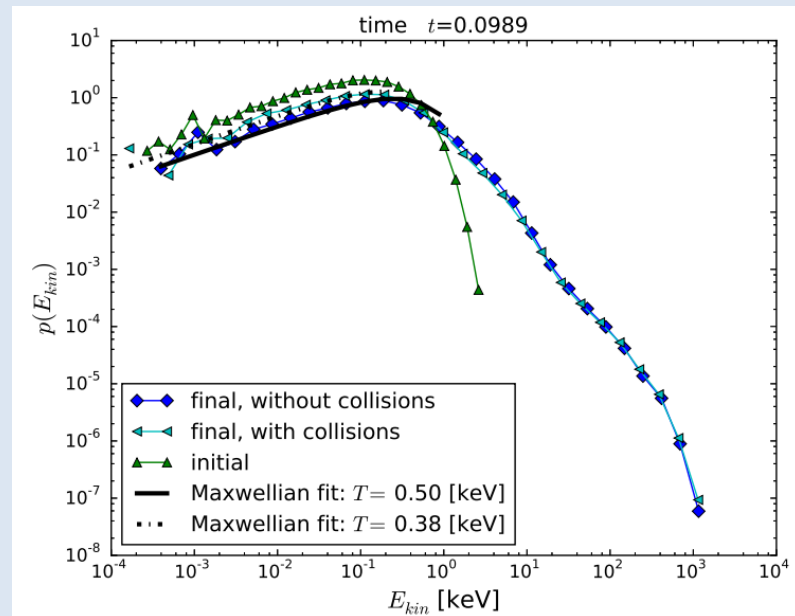
- 57% of the particles have left the system.
- Still power-law tail, **no clear scaling** anymore at higher energies (poor statistics due leaving particles)
highest energy reached **20 MeV (2MeV at 0.1s)**.
Heating to a temperature of 0.4 keV (0.5 keV at 0.1s),
- leaving particles: power-law tail similar as at 0.1 s,
low energy part is **closer to Maxwellian shape** ($T = 7.5 \text{ keV (28 MK)}$)



Standard jet: results at 0.1s

The effect of collisions:

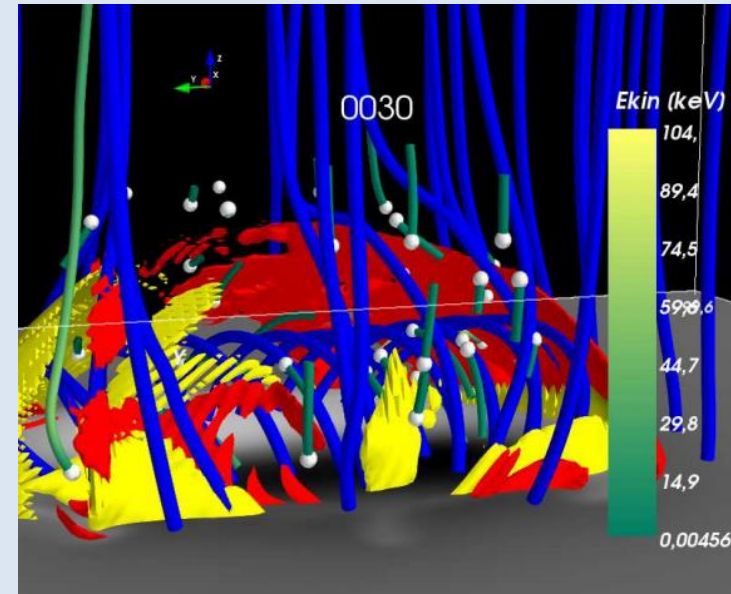
- collisions with background electrons of the same T as the initial T of the test-particles.
Collisions play a role at low energies only,
as expected, cooling down the electrons
- With collisions: **$T = 0.38$ keV,**
without collisions: **$T = 0.50$ keV.**
cooling down \rightarrow heating of the background



Standard jet: results at 0.1s

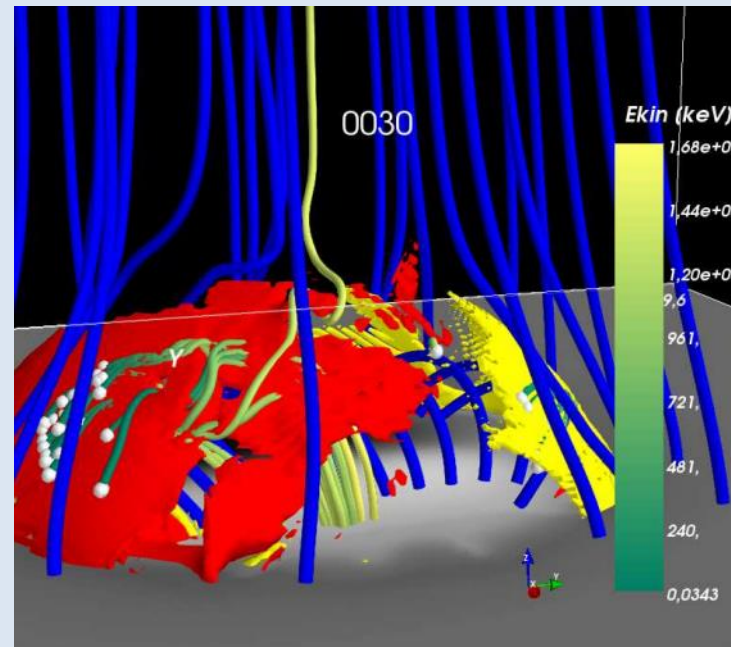
Orbits of 40 randomly chosen particles:

- shows population that is heated or moderately accelerated



orbits of the 40 most energetic particles:

- clear **preference in initial conditions:**
close to strong pos. and neg. parallel el. field.
- particles move some distance along E-field pass then through it at some point, whereby their energy increases strongly
- **Chosen threshold in parallel electric field out-lines region of most efficient acceleration**



Diffusion coefficients: the connection to Fermi acceleration and Fokker-Planck description

- The **Fokker-Planck equation (FPE)** in velocity space writes as

$$\partial f / \partial t = \nabla_{\mathbf{u}} \cdot [-\mathbf{D} \cdot \nabla_{\mathbf{u}} f + \mathbf{F} f]$$

and in cylindrical coordinates $\mathbf{u} = (u_{\perp}, u_{\parallel})$ it takes the form

$$\begin{aligned} \frac{\partial f}{\partial t} = & \frac{1}{u_{\perp}} \frac{\partial}{\partial u_{\perp}} u_{\perp} \left[-D_{\perp\perp} \frac{\partial f}{\partial u_{\perp}} - D_{\perp\parallel} \frac{\partial f}{\partial u_{\parallel}} + F_{\perp} f \right] \\ & + \frac{\partial}{\partial u_{\parallel}} \left[-D_{\parallel\perp} \frac{\partial f}{\partial u_{\perp}} - D_{\parallel\parallel} \frac{\partial f}{\partial u_{\parallel}} + F_{\parallel} f \right] \end{aligned}$$

- Time-dependent, velocity-space averaged transport coefficients**, where the average is over the sample of the test-particles,
- Note, we use **running estimate**, at predefined monitoring times t_k (Ragwitz and Kantz, PRL, 2001)

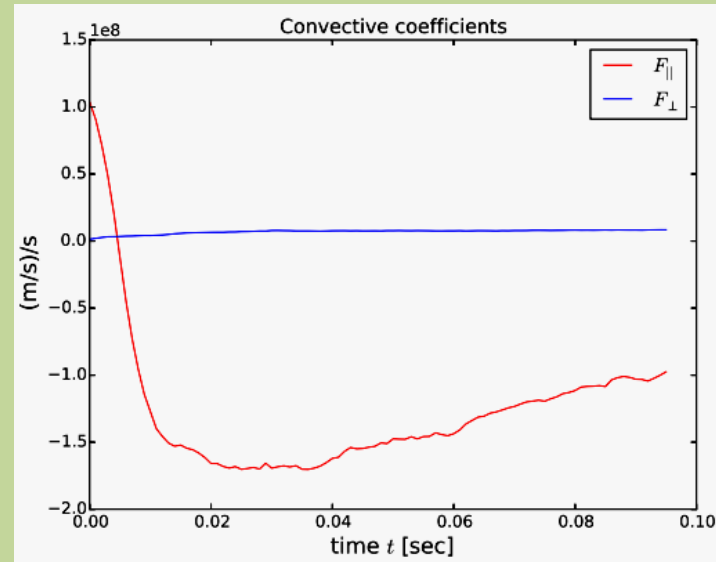
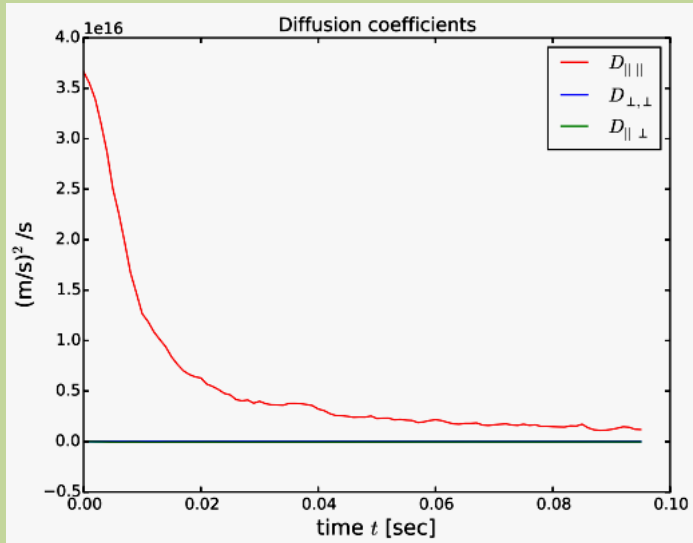
$$D_{\parallel\parallel}(t_k) = \frac{1}{2(t_{k+h} - t_k)} \langle (u_{\parallel}(t_{k+h}) - u_{\parallel}(t_k))^2 \rangle$$

$$F_{\parallel}(t_k) = \frac{1}{(t_{k+h} - t_k)} \langle (u_{\parallel}(t_{k+h}) - u_{\parallel}(t_k)) \rangle$$

→ seems a detail, but turned out to be important (e.g. when trying to reproduce the results of a classical random walk with the numerical solution of the FPE)

Time-dependent, velocity-space averaged transport coefficients

- Parallel diffusion/convection clearly dominates



- Yet, this picture is too simple, we have to consider the velocity dependence

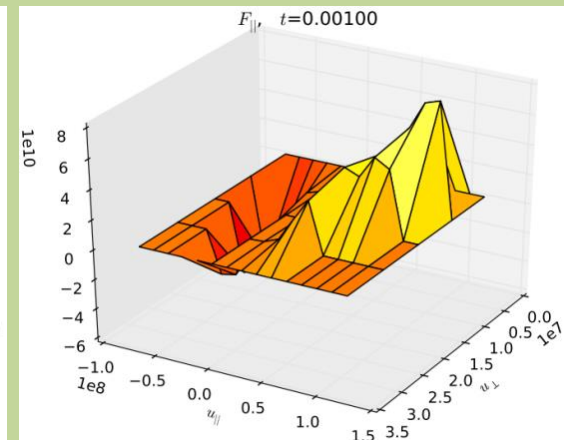
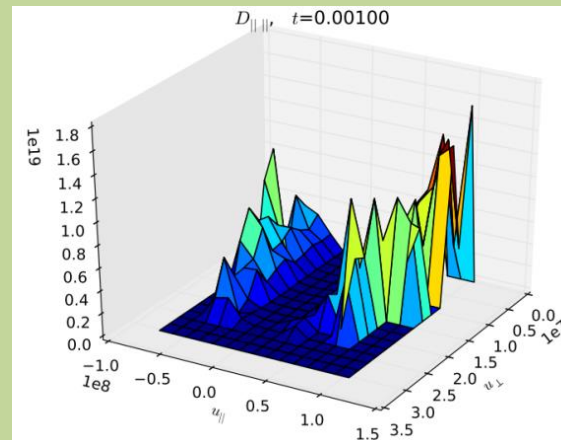
Time- and velocity-space-dependent transport coefficients

- An estimate of **the velocity-space- and time-dependence of the transport coefficients**, for given time t_k , can be made by
 - first prescribing **2D bins in the $u_{\perp} - u_{\parallel}$ - plane**, with mid-points $(u_{\perp,i}, u_{\parallel,j})$,
 - and then,, considering $[(u_{\parallel}^{(l)}(t_{k+h}) - u_{\parallel}^{(l)}(t_k))^2]$ a function of $(u_{\perp,i}, u_{\parallel,j})$ if $(u_{\perp}^{(l)}(t_k), u_{\parallel}^{(l)}(t_k))$ lies in the respective bin (i,j) for each particle, indexed with l ,
 - and do **binned statistics** to find the mean values such as

$$D_{\parallel\parallel}(t_k, u_{\perp,i}, u_{\parallel,j}) = \frac{1}{2(t_{k+h} - t_k)} \left\langle \left(u_{\parallel}^{(l)}(t_{k+h}) - u_{\parallel}^{(l)}(t_k) \right)^2 \right\rangle_l (t_k, u_{\perp,i}, u_{\parallel,j})$$

and the like for the other transport coefficients

- Quite noisy, nonetheless with clear structure in parallel direction:
 - **we can neglect the dependence on u_{\perp} !**

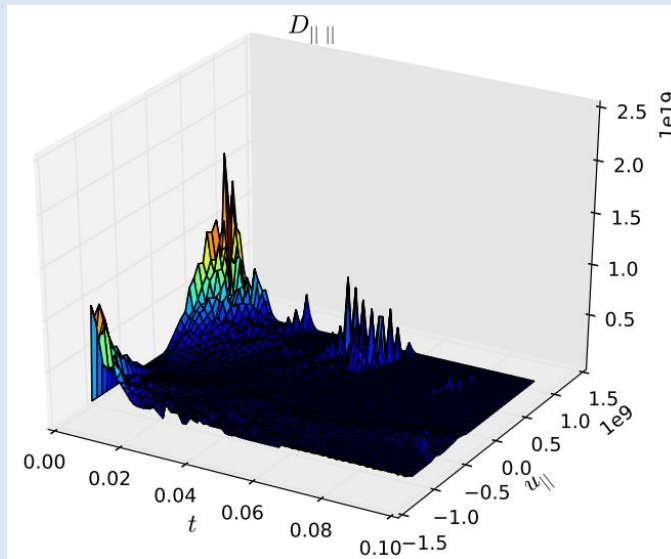


Time- and $v_{||}$ -dependent transport coefficients

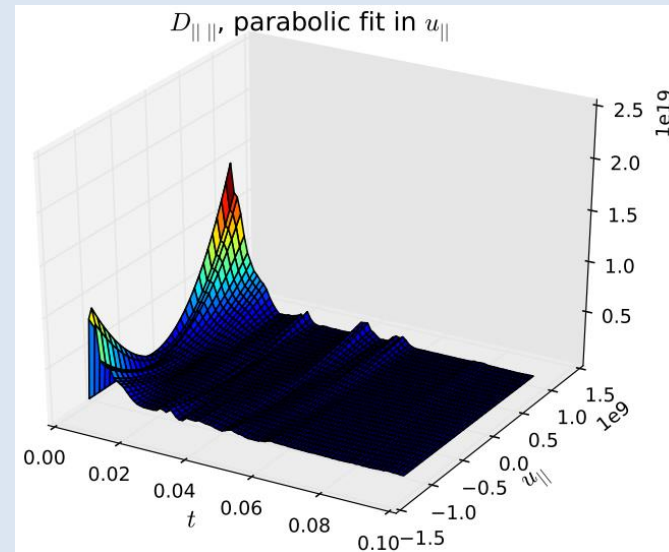
- **Diffusion coefficient:** We ignore the dependence on u_{\perp}

$$D_{||||}(t_k, u_{||,j}) = \frac{1}{2(t_{k+h} - t_k)} \left\langle \left(u_{||}^{(l)}(t_{k+h}) - u_{||}^{(l)}(t_k) \right)^2 \right\rangle_l (t_k, u_{||,j})$$

binned statistics



parabolic fit



- Some noise, yet **parabolic fit seems reasonable**, above all at small times

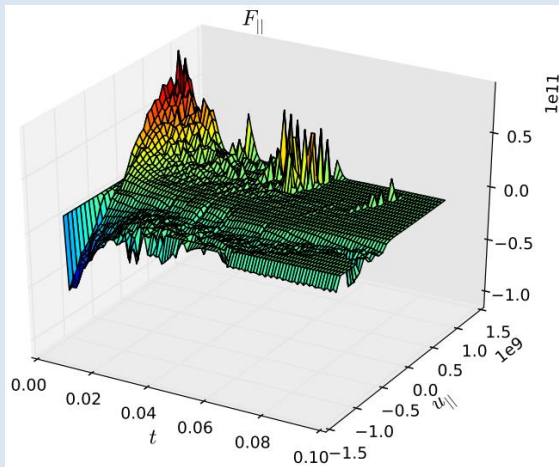
$$D_{||||}(t, u_{\perp}, u_{||}) \propto u_{||}^2 g(t)$$

Time- and $v_{||}$ -dependent transport coefficients

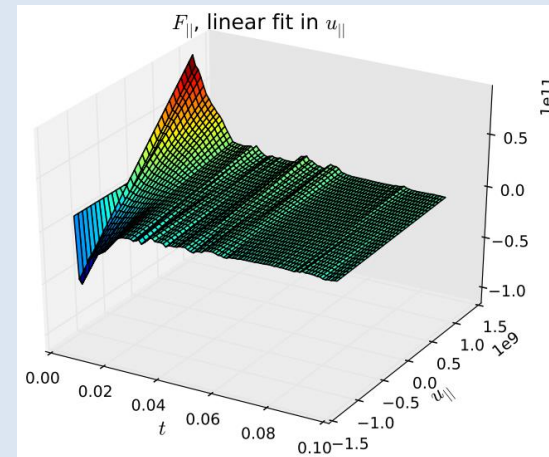
- **Convective coefficient:** We again ignore the dependence on u_{\perp}

$$F_{||||}(t_k, u_{||,j}) = \frac{1}{(t_{k+h} - t_k)} \left\langle \left(u_{||}^{(l)}(t_{k+h}) - u_{||}^{(l)}(t_k) \right) \right\rangle_l (t_k, u_{||,j})$$

binned statistics



linear fit



- Again, there is a lot of noise, yet the **linear fit seems more or less reasonable** at small times

$$F_{||}(t, u_{\perp}, u_{||}) = u_{||} g(t)$$

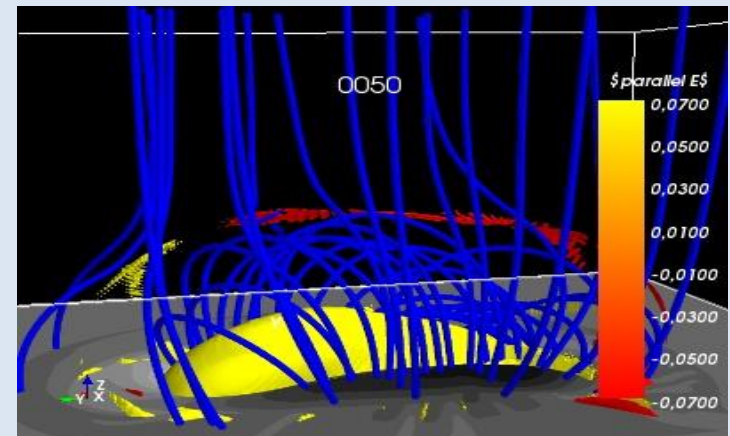
- $D_{||||}, F_{|||}$: **Basic dynamic acceleration takes place up to 0.02sec,**
 → particles have taken the energy that is available for them
 → there is a kind of **saturation effect**

Summary

- The MHD simulations yield various power-law distributions, and fractal structures, they are far from equilibrium
- For the test-particles, we find acceleration and heating. Both are a transient phenomenon, there is a kind of saturation effect
- Leaving particles form super-hot population, with power-law tail in energy
- The parallel dynamics clearly dominate the energetics
- transport coefficient are velocity-dependent, and seem to have simple functional form

Future steps:

- How are the various power-law indices related ?
- Analyze different MHD snapshots, e.g. with 'blowout jet'
- Spatial structure of E-field needs still to be further analyzed: e.g. Eulerian vs Lagrangian correlation.

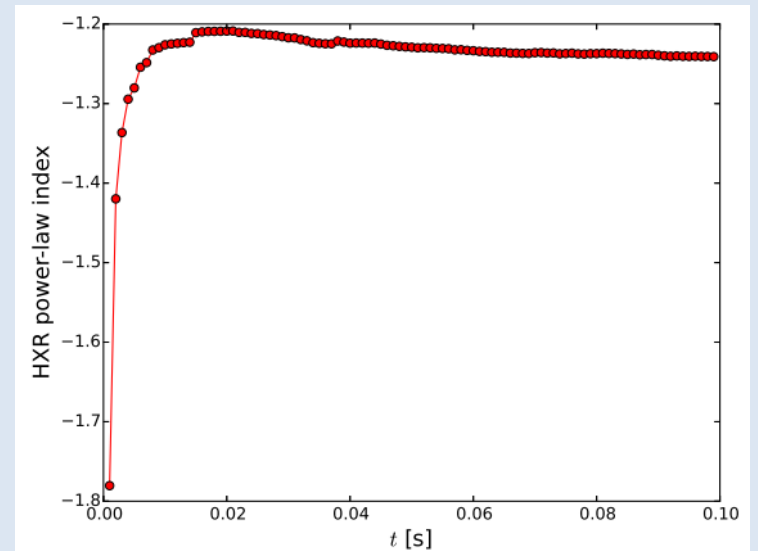
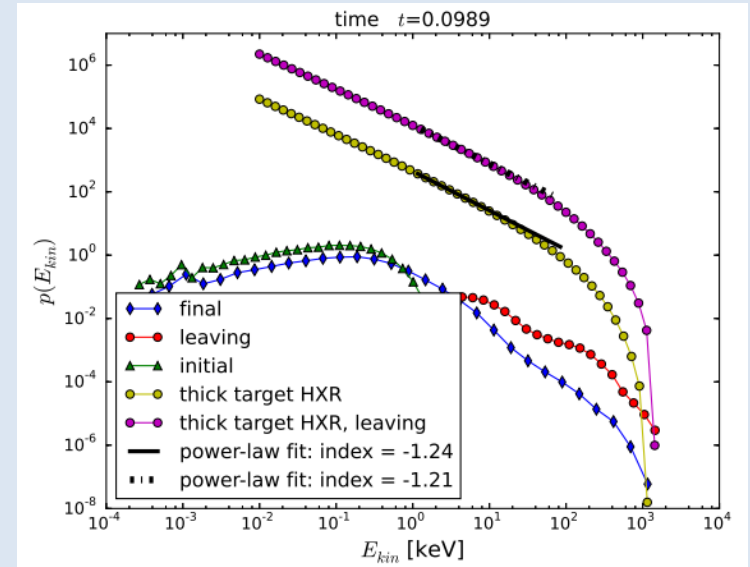


THE PRESENTATION ENDS HERE

Standard jet: results at 0.1s

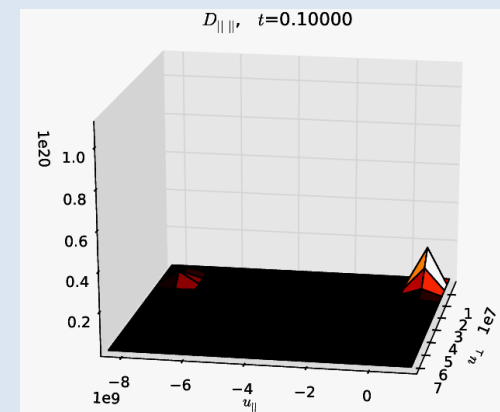
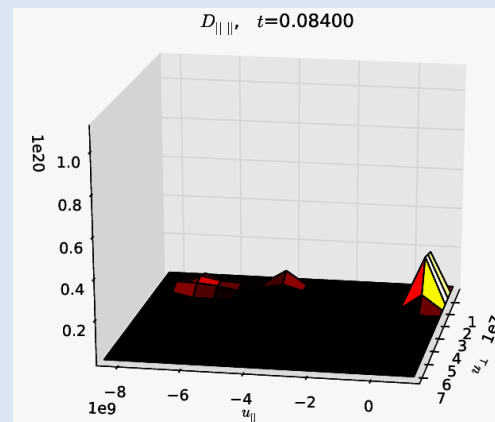
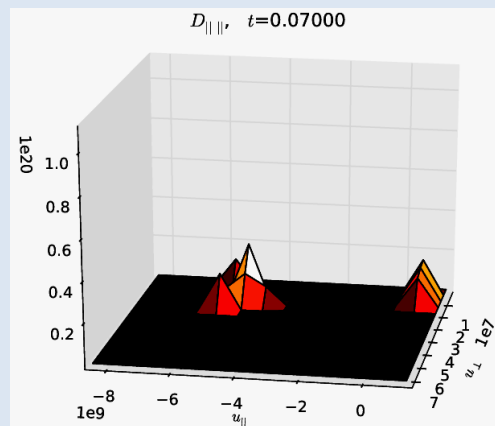
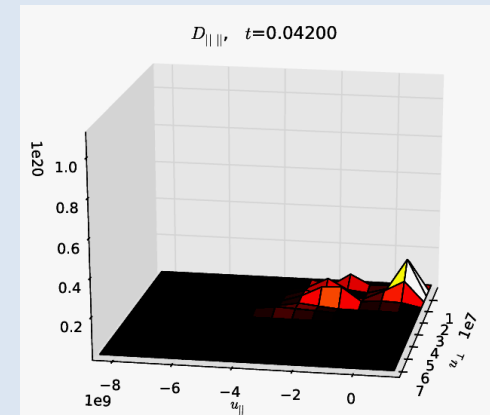
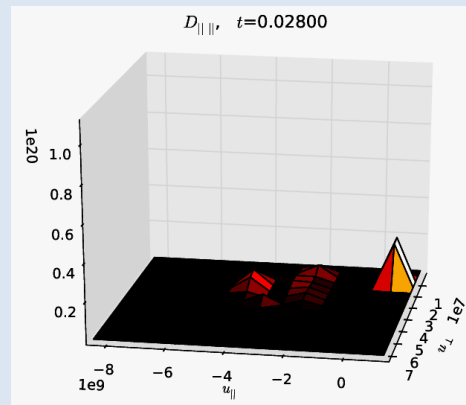
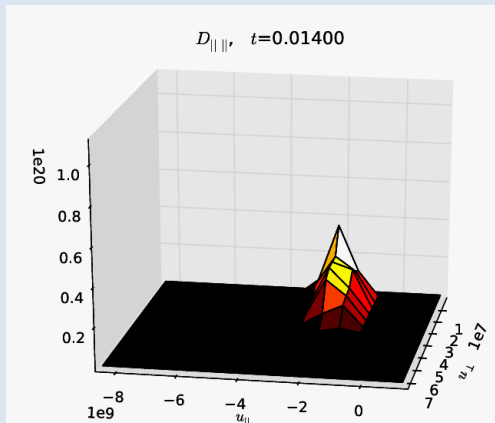
thick target HXR emission spectrum

- The HXR spectrum is rather flat, with **index** mostly close to **1.2**. HXR spectrum of the leaving particles is very similar in shape (asynchronous distribution !)
- the **time evolution of the power-law index** of the spectrum.



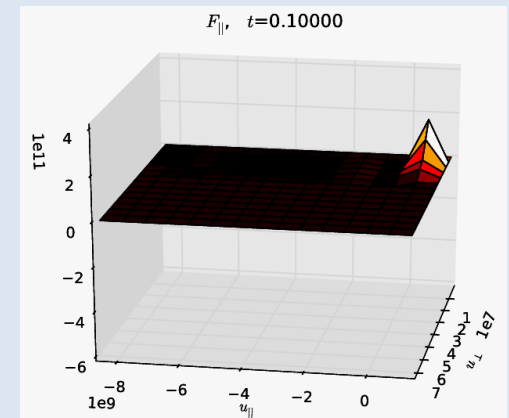
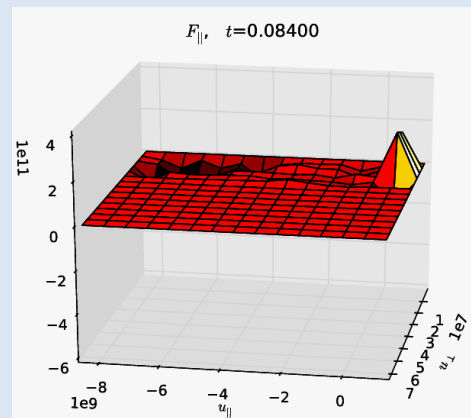
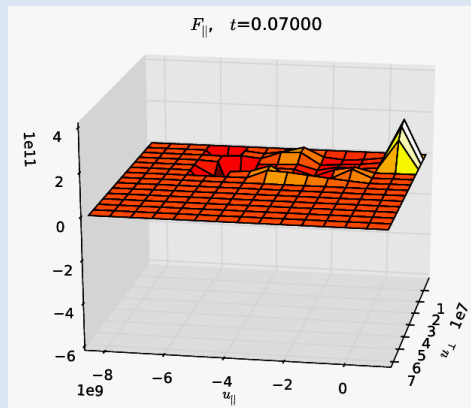
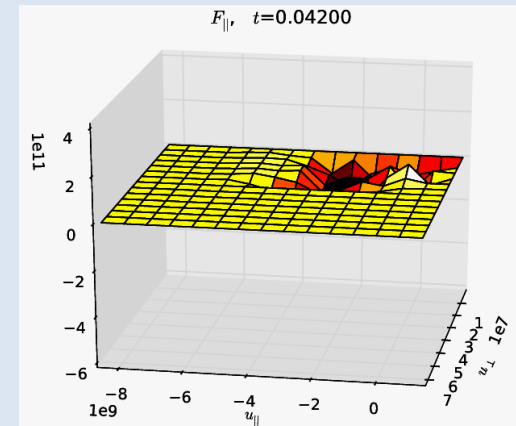
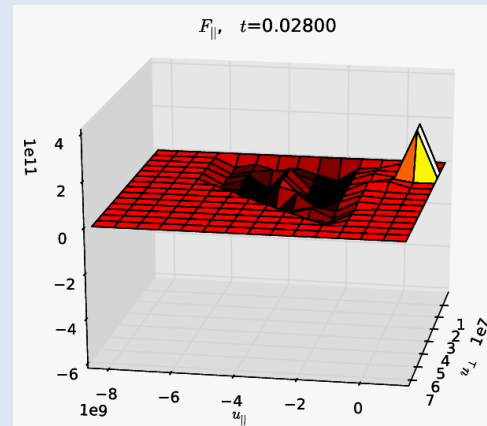
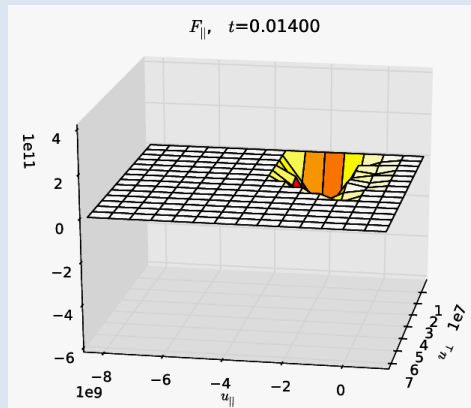
Time- and velocity-space-dependent transport coefficients

- Parallel diffusion coefficient $D_{\parallel\parallel}$
 - old result: $D_{\parallel\parallel}$ prop. to v_{\parallel}^2
 - clearly velocity dependent D , no obvious functional form, though



Time- and velocity-space-dependent transport coefficients

- Parallel convective coefficient $F_{||}$
 - old result $F_{||}$ prop to $v_{||}$
 - again: much less clear functional form now



Correct form of transport coefficients

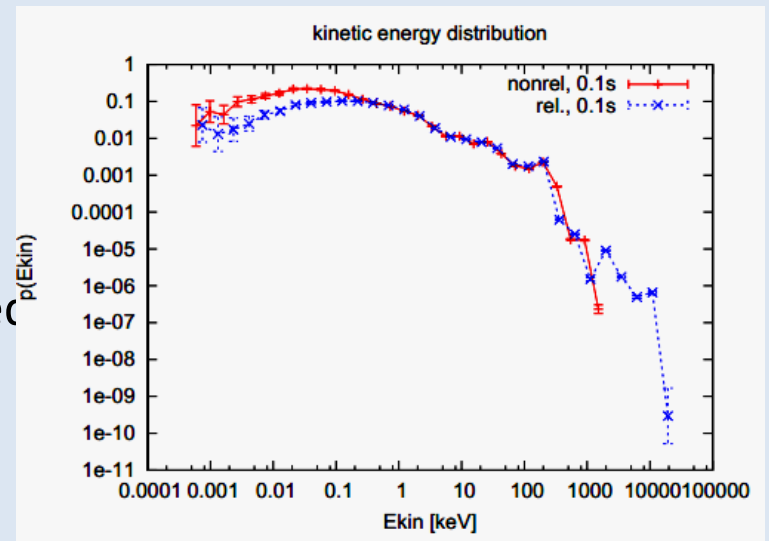
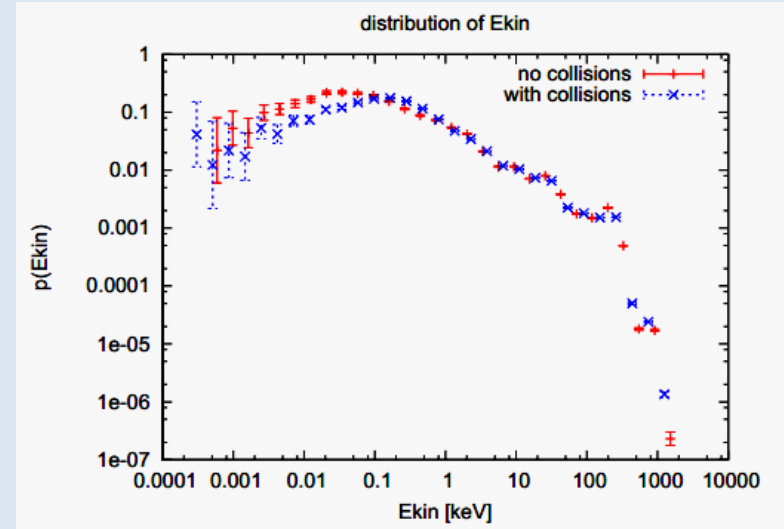
- is the form $D_{||}$ really correct,
i.e. will – in well behaved cases – the FPE yield the same as do the test-particle simulations ?
- We set up a simple random walk problem in 1D, with given step-size distribution for velocity and time, where $D_{||}$ can be derived analytically , and we estimate $D_{||}$ also numerically from the random walk:
The numerical $D_{||}$ gave distributions clearly different from the random walk
- **Corrected form of estimator for $D_{||}$** (and the other coefficients):
use running estimate, at predefined monitoring times t_k , and define

$$D_{||}(t_k) = \frac{1}{2(t_{k+h} - t_k)} \langle (v_{||}(t_{k+h}) - v_{||}(t_k))^2 \rangle$$

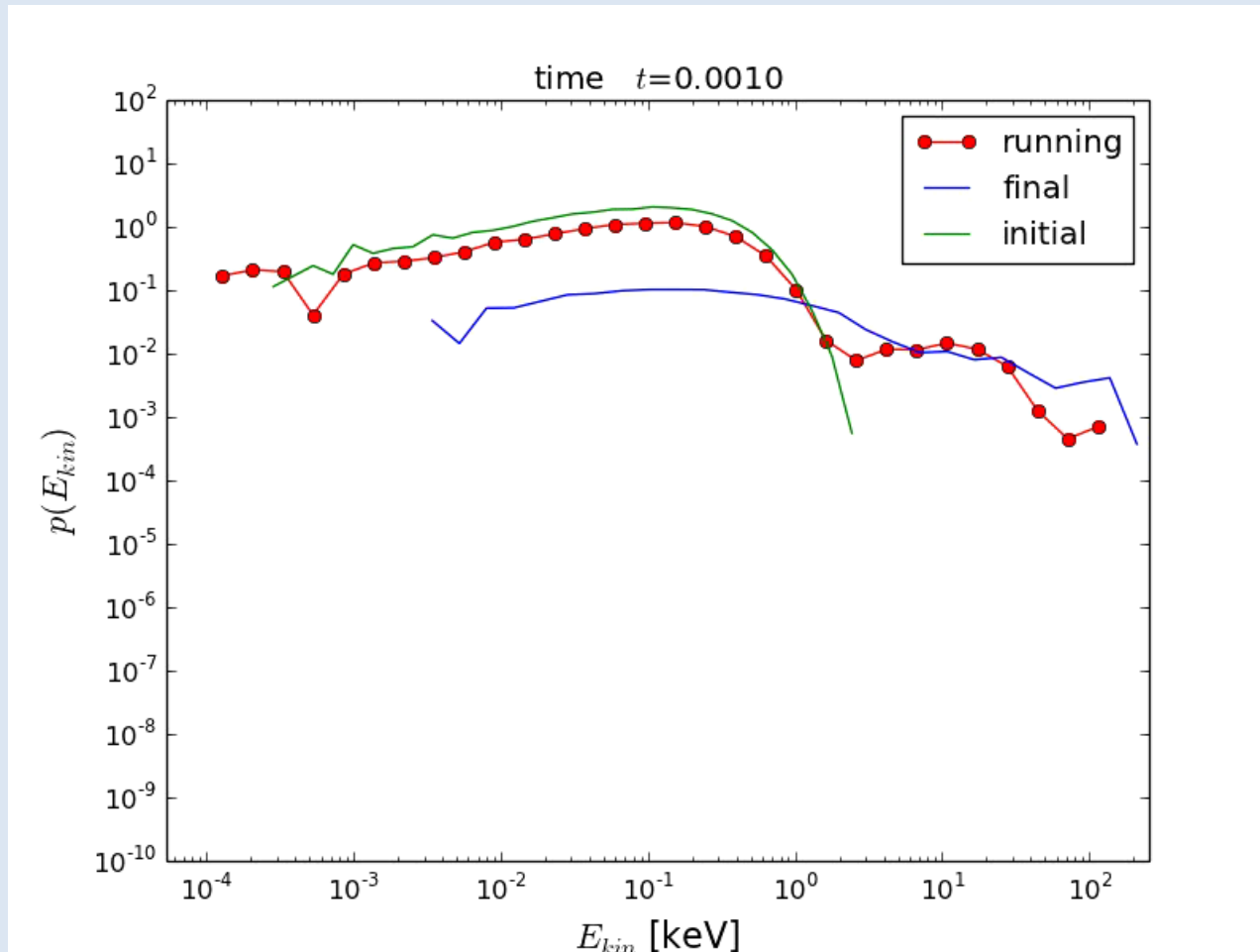
- numerical solution of FPE and random walk coincide very well !
→ seems a detail, but turned out to be important

The most explosive phase: collisions, relativistic effects

- **Collisions** (with background electrons) play a minor role at low energies
 - collisions can be neglected (Monte Carlo collision operator, Hamamatsu, K et al., Plasma Phys Contr Fus **49**, 1955 (2007))
- We consider **the relativistic equations** of guiding center motion, and compare with the non-relativistic case. In the relativistic case, the particles reach higher energies, in the intermediate to high energy range though, where a clear power-law is formed distribution is unaltered.
 - to be on the safe side, use relat. eqs.

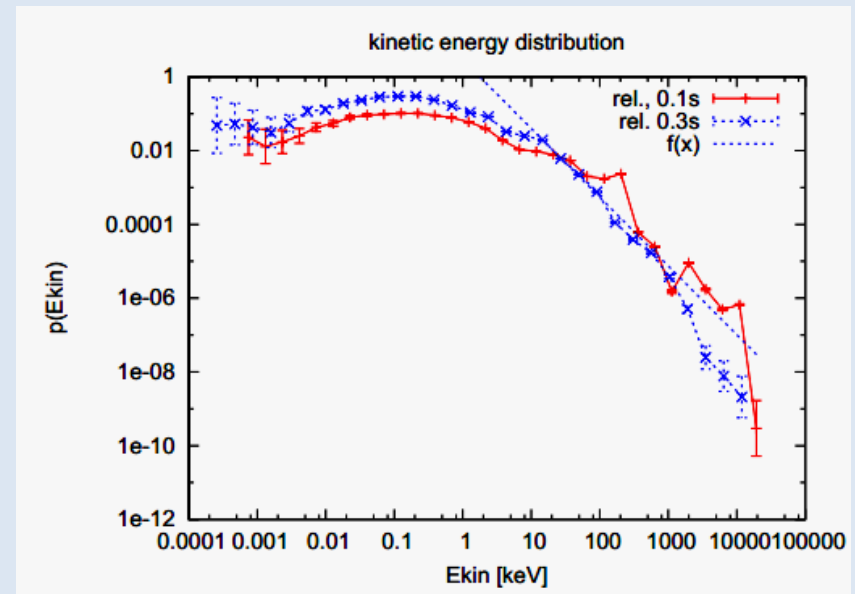


The most explosive phase



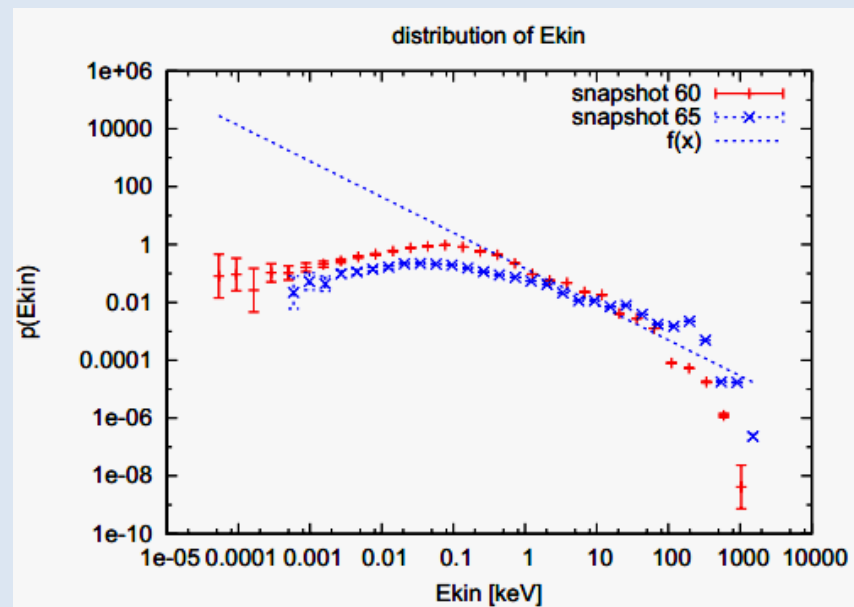
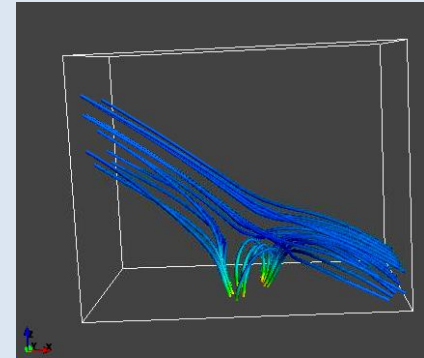
The most explosive phase: longer times

- We consider **the relativistic equations** of guiding center motion, for final times 0.1s and 0.3
 - The distributions **are similar in shape,**
 - at 0.3s the high energy part is **less noisy and shows now a clear power-law**
- A fit in the range [10,1000] yields an **index -1.9** (the fit is though not very good at the higher energies)



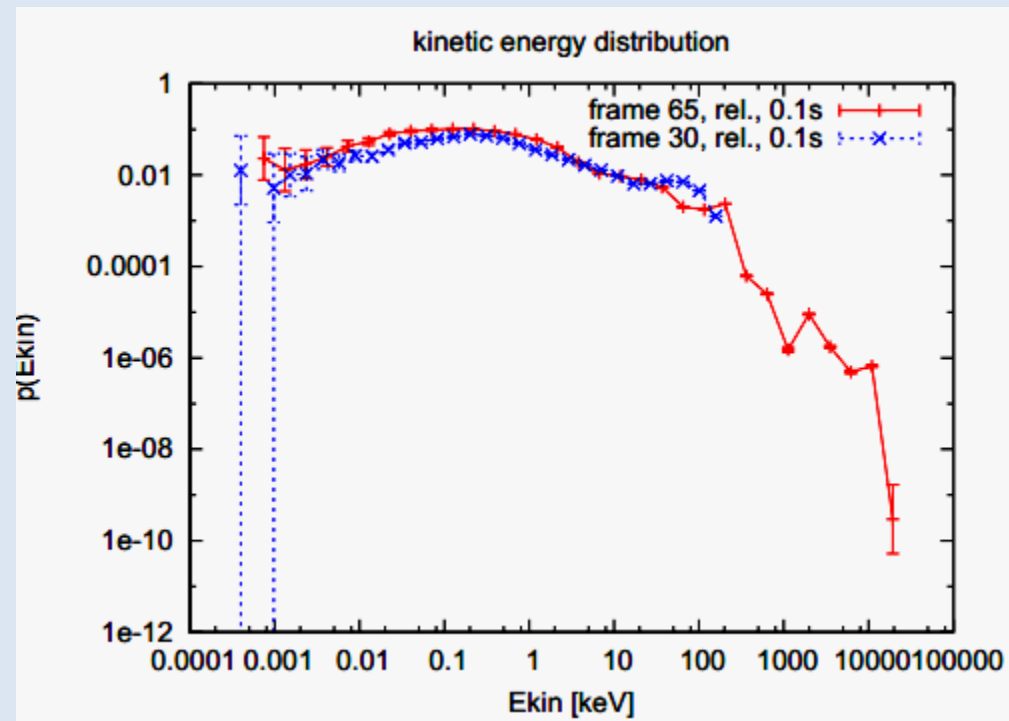
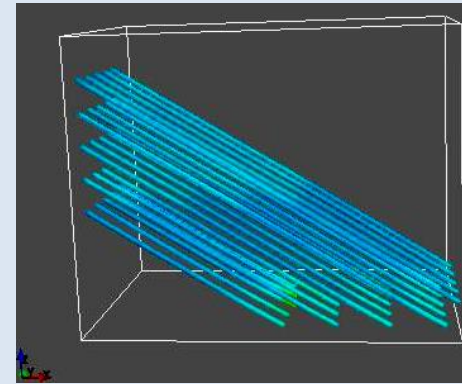
Before the most explosive phase

- We consider the **start of the blob formation**
- a fit in the range [0.4,80] yields a slope 1.2, i.e. the distribution is **steeper** (1.2 vs 0.6) in lesser developed turbulence, there seems to be less heating taking place at low energies



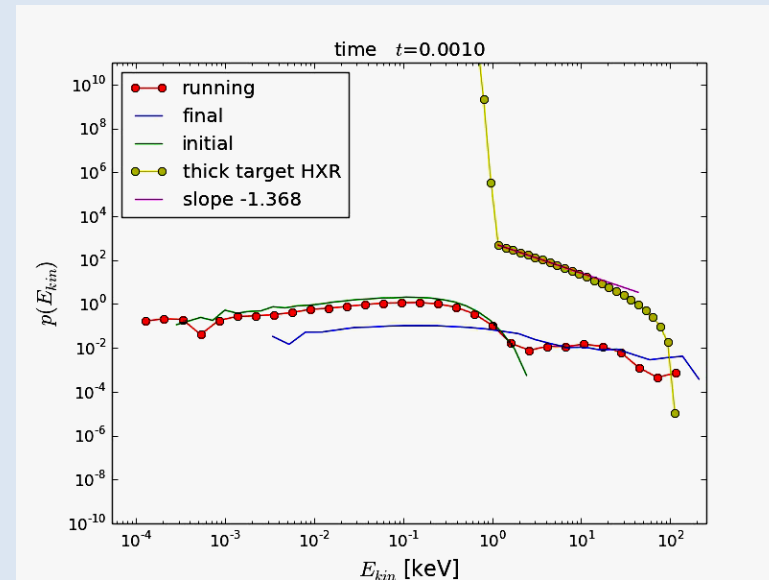
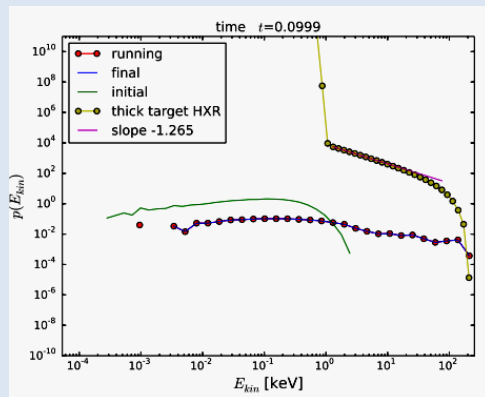
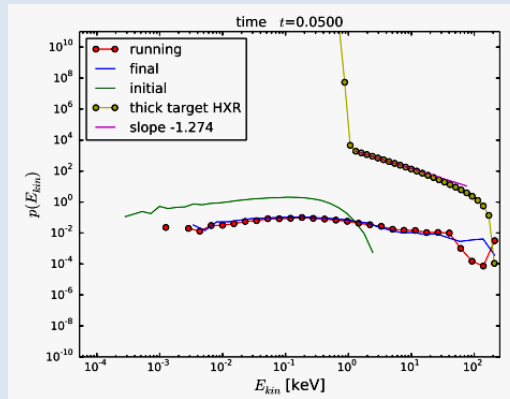
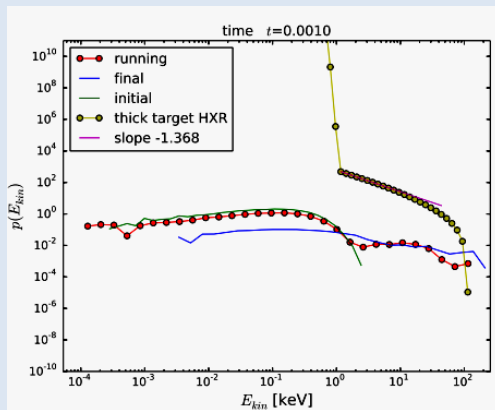
Initial, quiet phase

- snapshot 30 is far away from the blob formation, the coronal part still is rather **quiet**
- The highest energy reached, 150 keV, is much smaller than in developed turbulence
- up to 150keV the distributions are very similar, **heating is similar in both MHD time instances**



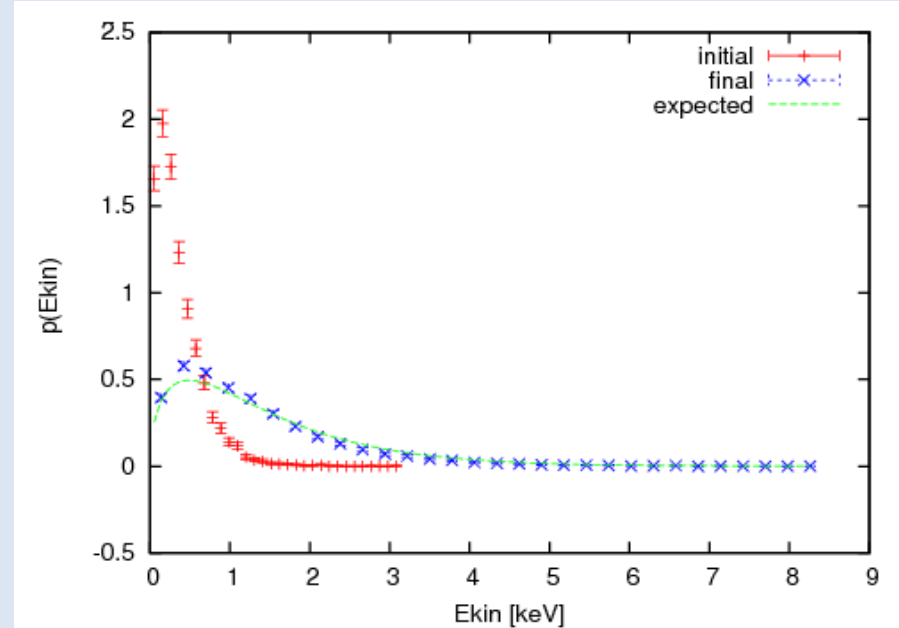
The most explosive phase: HXR emission

- Assuming that the particles instantaneously would precipitate onto the lower corona, we calculate **the thick target HXR spectrum** from the energy distribution (Brown, Holman)
- HXR emission at **three different times**:
The HXR spectrum is rather flat (**slope 1.2 to 1.4**).



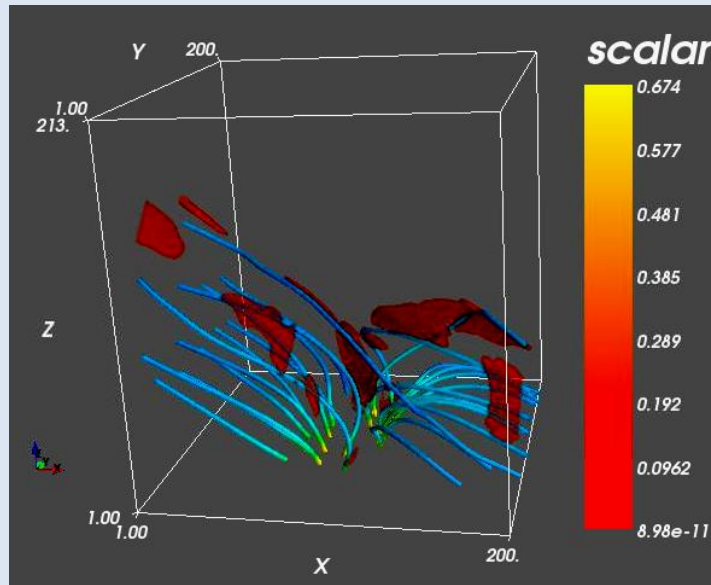
Collisions: benchmark

- We use the **Monte Carlo collision operator** as described in Hamamatsu, K et al., Plasma Phys Contr Fus **49**, 1955 (2007): random walk steps super-imposed on deterministic motion, after time intervals related to the collision time
- Particles collide with a **Maxwellian background**
- **Benchmark:** ions colliding with background electrons that have 4 times larger temperature than the ions initially:
Final ion distribution well coincides with expected distribution, the ions are heated (after 300 sec, with collision time = 0.3 sec)



Spatial structure of the magnetic and electric field (2/2)

- Magnitude of **parallel electric field** also fragmented (dominantly responsible for acceleration, see later)



- Fragmentation needs to be quantified: **cluster analysis, fractal dimension:** work in progress

Summary of older results, presented in Ioannina

- **Collisional effects** are not important
- **Relativistic equations of motion** should be used (the particles reach higher energies)
- **Longer integration times** lead to more well formed power-laws
- During explosive MHD phases, there is **heating and acceleration**, during quiet phases, there is **only heating**
- calculating **the thick target HXR spectrum** from the we find so-far that the HXR spectrum is rather flat.
- **Scaling factor for E** is necessary and strongly affects the results